and accurate to serve as a convenient, although approximate, alternative for optical diffraction experiments or numerical simulations of more complicated systems with more than one scattering object in the unit cell and with form factors taken into account.

This study was supported by the Netherlands Organization for the Advancement of Pure Research (NWO).

References

COWLEY, J. M. (1984). *Difraction Physics.* Amsterdam: North-Holland.
HOSEMANN, R. (1975). *J. Polym. Sci.* **50**, 265-281.
HOSEMANN, R. & BAGCHI, S. N. (1962). *Direct Analysis of Diffraction by Matter.* Amsterdam: North-Holland.
KITTEL, C. (1976). *Introduction to Solid State Physics.* New York: John Wiley.
MCWEENY, R. (1952). *Acta Cryst.* **5**, 463-468.
MCWEENY, R. (1953). *Acta Cryst.* **6**, 631-637.
SHAVITT, I. (1963). *Methods Comput. Phys.* **2**, 1-45.
THAKUR, M., TRIPATHY, S. K., BURKHART, C. W. & LANDO, J. B. (1985). *Acta Cryst.* A**41**, 30-34.
THAKUR, M., TRIPATHY, S. K. & LANDO, J. B. (1985). *Acta Cryst.* A**41**, 26-30.
WARREN, B. E. (1955). *Acta Cryst.* **8**, 483-486.
WARREN, B. E. & AVERBACH, B. L. (1950). *J. Appl. Phys.* **21**, 595-599.
WELBERRY, T. R. (1985). *Rep. Prog. Phys.* **48**, 1543-1593.
WELBERRY, T. R. & CARROLL, C. E. (1982). *Acta Cryst.* A**38**, 761-772.
WELBERRY, T. R. & CARROLL, C. E. (1983). *Acta Cryst.* A**39**, 233-245.
WELBERRY, T. R., MILLER, G. H. & CARROLL, C. E. (1980). *Acta Cryst.* A**36**, 921-929.
YU, L. C., STEVEN, A. C., NAYLOR, G. R. S., GAMBLE, R. C. & PODOLSKY, R. J. (1985). *Biophys. J.* **47**, 311-321.

Acta Cryst. (1989). A**45**, 870-878

Quantitative Determination of Phases of X-ray Reflection from Three-Beam Diffraction. III. Experiments on Mosaic Crystals

BY SHIH-LIN CHANG, MAU-TZAI HUANG AND MAU-TSU TANG

Department of Physics, National Tsing Hua University, Hsinchu, Taiwan 30043

AND CHIH-HAO LEE

Synchrotron Radiation Research Center, Hsinchu, Taiwan 30043

(*Received* 18 *July* 1989; *accepted* 10 *August* 1989)

Abstract

The method proposed by Chang & Tang [*Acta Cryst.* (1988), A**44**, 1065-1072] for quantitative determination of phases of X-ray reflection from three-beam diffraction profiles is applied to an organic crystal of (2*R*, 3*R*)-3-acetoxy-5,7-dihydroxy-6-methylflavanone, with a mosaic spread of 0·08°. The expression for the kinematical diffraction intensities is modified according to the kinematical theory of X-ray diffraction in the multibeam regime. Three-beam *Umweganregung* and *Aufhellung* diffraction profiles are analyzed. With the help of the modified intensity expression, the crystal symmetry imposed by the space group and the three-beam diffraction geometry, four acentric phases and fourteen centric phases of structure-factor triplets are determined.

I. Introduction

A theoretical consideration of quantitative phase determination using three-beam multiple diffraction has recently been reported (Chang & Tang, 1988). Phase determination for diffractions from perfect crystals was also demonstrated subsequently (Tang & Chang, 1988). These two reports are hereafter referred to as papers I and II in the following discussions. In paper I, a general formalism was derived from the dynamical theory of X-ray diffraction. The first-order approximation in the iterative procedure for the fundamental equation of the wavefield was adopted for *Umweganregung* three-beam diffractions, where the multiple diffracted intensity is greater than the two-beam intensity background. Boundary conditions were considered for plate-like crystals. For *Aufhellung* three-beam diffractions, where the multiple diffraction intensity is lower than the two-beam background, a second-order approximation was proposed to deduce the expressions for diffraction intensities. In paper II, the experiments for plate-like perfect crystals of GaAs demonstrated the possibility of determining quantitatively the phases of acentric reflections.

In mosaic crystals, lattice perfection is not guaranteed. According to Zachariasen (1945), diffractions

0108-7673/89/120870-09$03.00

from mosaic crystals have the magnitude of the parameter A much less than unity. The parameter A is defined as

$$A = r_e\lambda T|F_G|/(V\gamma_0^{1/2}\gamma_G^{1/2}) \quad (1)$$

where r_e and λ are the classical radius of the electron and the wavelength of the X-rays used, respectively. V is the volume of the unit cell and γ_0 and γ_G are the direction cosines of the incident beam 0 and the diffracted beam G with respect to the inward normal to the crystal surface. F_G is the structure factor of the G reflection in two-beam cases. In multibeam cases, F_G stands for the effective structure factor (Juretschke, 1982; Hoier & Marthinsen, 1983). T is the crystal thickness. The smallness of A, *i.e.* $A \ll 1$, implies that the coherent dynamical interaction, which carries phase information, is relatively weak. On the other hand, extinction, mainly secondary extinction, affects considerably the kinematical diffraction intensity, while irregular crystal shape imposes complicated boundary conditions for dynamical excitation. All of these introduce difficulties in delineating the dynamical intensity profile from the intensity measurements. It is the purpose of this paper to demonstrate how to combine the three-beam kinematical theory with the dynamical theory so as to separate the contribution of the dynamical diffraction from the kinematical diffraction and consequently to bring out phase information from the weak dynamical diffraction intensities for mosaic crystals.

In the literature, experimental phase determination using X-ray multiple diffraction techniques for mosaic crystals has been reported by Post (1977), Jagodzinski (1980), Chang (1982), Han & Chang (1983), Gong & Post (1983), Shen & Colella (1988), Mo, Hauback & Thorkildsen (1988), Hümmer, Weckert & Bondza (1989) and many others. Detailed references on this subject matter can be found in the review article of Chang (1987).

II. Theoretical considerations

Consider a three-beam (0, G, L) diffraction in which 0 is the incident diffraction and G and L are the primary and the secondary reflections, respectively. $G-L$ is the coupling between G and L. Recall the recurrent relation, equation (9) of paper I, of the wavefield amplitude $\mathbf{D}_G$ of the G reflection:

$$\begin{aligned}\mathbf{D}_G = {} & A_G\chi_G\mathbf{K}_G\times\mathbf{K}_G \\ & \times\{\mathbf{D}_0 + A_L(\chi_{G-L}/\chi_G)[\chi_L\mathbf{K}_L\times(\mathbf{K}_L\times\mathbf{D}_0) \\ & + \chi_{L-G}\mathbf{K}_L\times(\mathbf{K}_L\times\mathbf{D}_G)]\}, \end{aligned} \quad (2)$$

where

$$A_G = 1/[(k^2 - K_G^2) + K_G^2\chi_0] \quad (3)$$

$$A_L = 1/[(k^2 - K_L^2) + K_L^2\chi_0]. \quad (4)$$

The quantity $\chi_{G-L}/4\pi$ is the electric susceptibility of the $G-L$ reflection, which is proportional to the structure factor F_{G-L}:

$$\chi_{G-L} = \Gamma F_{G-L} = -(\gamma_e\lambda^2/\pi V)F_{G-L}. \quad (5)$$

k and K are the moduli of the wavevectors in vacuum and inside the crystal, respectively.

According to the theorem of reciprocity of optics, it is known that the interchange of the L and $G-L$ reflections leads to no difference in the wavefield amplitude D. In other words, the two three-beam cases, (0, G, L) and (0, G, $G-L$), are equivalent (Pinsker, 1977; Chang 1984). However, in the approximation for iteration, the $\mathbf{D}_G$ of (2) violates this theorem of reciprocity because of the presence of the last term in (2). In paper I, we have employed the first-order approximation, where the last term of (2) was dropped, so that the reciprocity is maintained. The relative intensity distribution of the primary reflection G, after the convolution with the crystal mosaic distribution and the instrumental broadening, can be expressed as a function of the azimuthal angle of φ of rotation around the reciprocal-lattice vector $\mathbf{g}$ of the G reflection (Chang & Tang, 1988):

$$I'_G = [I_G(3) - I_G(2)]/I_G(2) = I_D + I_K, \quad (6)$$

where $I_G(2)$ and $I_G(3)$ are the diffracted intensities of the G reflection at the two-beam and the three-beam positions, respectively. The dynamical intensity I_D and the kinematical intensity I_K are defined as

$$I_D = 2Pa_1Q[2(\Delta\varphi)\cos\delta - \eta_T\sin\delta] \quad (7)$$

$$I_K = a_2\eta_T P^2/\eta_i \quad (8)$$

where

$$P = |\Gamma|kL_FQ(|F_{G-L}||F_L|/|F_G|) \quad (9)$$

$$Q = 1/[(\Delta\varphi)^2 + (\eta_T/2)^2]^{1/2} \quad (10)$$

$$W = kl\sin\alpha\sin\beta_0\cos\theta_G \quad (11)$$

$$\eta_T = \eta_i + \eta_B + \eta_M \quad (12)$$

$$\eta_i = k^2|\chi_0|/W. \quad (13)$$

a_1 and a_2 are the polarization factors defined as

$$a_1 = (B_0 + B_5\cos 2\theta_G)p_2 \quad (14)$$

$$a_2 = (B_0^2 + B_3^2 + B_4^2 + B_5^2)p_2 \quad (15)$$

where

$$\begin{aligned} B_0 &= 1 - (l/k)^2\sin^2\alpha\sin^2\beta_0 \\ B_3 &= (l/k)\sin\alpha\sin\beta_0[(l/k)\sin\alpha\cos\beta_0\sin\theta_G \\ &\quad + (l/k)\cos\alpha\cos\theta_G - \sin 2\theta_G] \\ B_4 &= (l/k)^2(\cos\alpha\cos\theta_G \\ &\quad - \sin\alpha\cos\beta_0\sin\theta_G)\sin\alpha\sin\beta_0 \\ B_5 &= \cos 2\theta_G - B_3B_4/[(l/k)\sin\alpha\sin\beta_0]^2 \\ p_2 &= 1/(1+\cos^2 2\theta_G). \end{aligned}$$

δ is the phase of the structure-factor triplet $F_G F_L F_{G-L}$. η_T is the total experimental width at half maxima. η_i, η_B and η_M are the intrinsic diffraction width, the average instrumental broadening and the crystal mosaic spread, respectively. $\Delta\varphi$ is the angular deviation from the exact three-beam diffraction position. L is the Lorentz factor defined as k/W. l is the modulus of the reciprocal-lattice vector $\mathbf{l}$ of the L reflection. θ_G and α are the Bragg angle of the G reflection and the angle between the vectors $\mathbf{g}$ and $\mathbf{l}$. β_0 is the angle between $\mathbf{l}_\perp$ and the plane of incidence, where $\mathbf{l}_\perp$ is the vector component of $\mathbf{l}$ normal to $\mathbf{g}$. For a plate-like crystal, η_i can be written as [see equation (35) of paper I]

$$\eta_i = k|L_F|(\gamma_L/\gamma_0)|\chi_0|, \tag{16}$$

where γ_0 and γ_L are the direction cosines. For a crystal of arbitrary shape, we introduce a factor C_1 in η_i to take care of the boundary conditions for wavevectors:

$$C_1\eta_i = C_1 k|L_F\chi_0|. \tag{17}$$

The approximation for the wavefield amplitudes employs an iteration procedure. This approach is the same as the second-order Bethe approximation (Høier & Marthinsen, 1983; Juretschke, 1982; Hümmer & Billy, 1986) and the Born approximation (Shen, 1986), except that the resonance function A_L of (4) has been introduced to describe the intensity at the peak position. Actually, (6) can also be derived from the Bethe approximation and the Born approximation. On the other hand, I_K given in (8) has exactly the same form as that derived from the kinematical theory for *Umweganregung* diffraction for a weak primary reflection (Moon & Shull, 1964). Physically, this procedure, valid up to first-order approximation, is not in a strict manner consistent with the 'simultaneous' nature of multiple diffraction. To consider the simultaneous occurrence of diffractions and the kinematical diffractions from mosaic crystals, the kinematical intensity I_K is replaced by the expression derived from the power-transfer equation of the kinematical theory (Moon & Shull, 1964). With a modified coefficient keeping the dimension of I_K the same as that given in (8), the kinematical intensity takes the form

$$I_{K,T} \simeq (\eta_T/\eta_i)k^2\Gamma^2 L_F^2 Q^2 R \tag{18a}$$

with

$$R = [a_2|F_{G-L}|^2|F_L|^2 - a_3|F_G|^2|F_L|^2 - a_4|F_G|^2|F_{G-L}|^2]/|F_G|^2, \tag{18b}$$

where the polarization factors a_3 and a_4 are defined as

$$a_3 = [\cos^2 2\theta_G + \cos^2 2\theta_L + (\cos 2\theta_{G-L} - \cos 2\theta_G \cos 2\theta_L)^2]p_2 \tag{19a}$$

$$a_4 = [\cos^2 2\theta_G + \cos^2 2\theta_{G-L} + (\cos 2\theta_L - \cos 2\theta_G \cos 2\theta_{G-L})^2]p_2. \tag{19b}$$

θ_L and θ_{G-L} are the Bragg angles of the L and $G-L$ reflections, respectively. Equation (18a) reduces to (8) as F_G approaches zero. Both (18a) and (8) are valid for weak reflections with $ql_0 < 1$ and $\mu l_0 < 1$, where q is the reflectivity defined as

$$q_G = (r_e^2\lambda^3/V^2)|F_G|^2(1+\cos^2 2\theta)/(2\sin 2\theta_G). \tag{20}$$

μ and l_0 are the linear absorption coefficient and the X-ray path length, respectively.

In practice, the experimental kinematical intensity I_K is different from the theoretical $I_{K,T}$ given in (18) due to (i) the error of the resonance function A_L introduced in the iterative procedure, and (ii) the extinctions. For an irregularly shaped crystal, the intensity ratios, $I_K/I_{K,T}$ at $\Delta\varphi = 0$, are almost constant for the three-beam diffractions involving approximately the same kinematical intensities, because the effects of the extinctions and the errors in the theoretical approximations are almost the same. Under this condition, we could assume that

$$I_K = C_0 I_{K,T} \tag{21}$$

for a set of three-beam diffractions which have similar $I_{K,T}$ values. If very weak three-beam diffractions are considered (*i.e.* $ql_0 < 1$, $\mu l_0 < 1$), both the primary and secondary extinctions are small. The $I_{K,T}$ given in (18a) is suited for calculating the kinematical intensities.

To determine the scale factor C_0, we consider the ratio of $I_{K,T}$ and the experimental intensity of I'_G, at the peak position, $\Delta\varphi = 0$, *i.e.* $I_P = I'_G(\Delta\varphi = 0)$, as

$$I_P/I_{K,T}(0) = [I_D(0) + I_K(0)]/I_{K,T}(0) = \pm 4P(0)a_1 \sin\delta/I_{K,T}(0) + C_0, \tag{22}$$

where the relations (6), (7) and (8) have been used. The plus and minus signs correspond to the *Umweganregung* and the *Aufhellung* diffractions, respectively. If a three-beam diffraction with $\delta = 0$ or 180°, the C_0 can be determined *via* the $I_P/I_{K,T}(0)$. Thus, the determined C_0 can be used to calculate the I_K from (21) for the other reflections which have similar $I_{K,T}$ values.

From (22), we notice that if $\delta > 0$ and $a_1 > 0$, $I_P/I_{K,T}(0) < C_0$ for *Umweg* and $I_P/I_{K,T}(0) > C_0$ for *Aufhellung*. If $\delta < 0$ and $a_1 > 0$, the situations are reversed for *Umweg* and *Aufhellung*.

It should be noted that the $\Delta\varphi$ in the first term of (7) involves the sign of L_F, which is defined as (Chang & Tang, 1988)

$$S(L_F) = S \pm S_{GL}, \tag{23}$$

where $S_\pm$ is positive for the 'IN' position φ_+ at which the reciprocal-lattice point L is entering the Ewald sphere; $S_\pm$ is negative for the 'OUT' position φ_- at which the reciprocal-lattice point L is leaving the Ewald sphere. S_{GL} is the sign of $l^2 - \mathbf{l}\cdot\mathbf{g}$ (Shen, 1986). That is, the sign of cos δ to be determined *via* (7)

depends on $S(L_F)$, while the sign of $\sin\delta$ is independent of $S(L_F)$.

With the determined C_0 factor, the measured η_T, the calculated η_i, a_2, a_3, a_4, and the structure-factor amplitudes deduced from two-beam intensity measurements, the kinematical diffraction profile $I_K(\Delta\varphi)$ can be calculated as

$$I_K(\Delta\varphi) = C_A \mathscr{L}(\Delta\varphi) \tag{24}$$

where

$$C_A = C_0 \Gamma^2 k^2 L_F^2 (\eta_T/\eta_i) R \tag{25}$$

$$\mathscr{L}(\Delta\varphi) = Q^2. \tag{26}$$

$\mathscr{L}$ is a Lorentzian. The azimuthal position φ_+ or φ_- at the exact three-beam point, $\Delta\varphi = 0$, is the center of the Lorentzian. $\varphi_\pm$ can be calculated according to the diffraction geometry (Cole, Chambers & Duun, 1962; Chang & Tang, 1988). The dynamical diffraction profile $I_D(\Delta\varphi)$ is then equal to $I_D(\Delta\varphi) = I'_G(\Delta\varphi) - I_K(\Delta\varphi)$. The phase angle δ for $a_1 L_F > 0$ can be determined according to the relations (Chang & Tang, 1988)

$$\cos\delta - \sin\delta = I_+/(2Pa_1QW)|_{\Delta\varphi=\eta_T/2} \tag{27a}$$

$$-\cos\delta - \sin\delta = I_-/(2Pa_1QW)|_{\Delta\varphi=\eta_T/2,} \tag{27b}$$

where

$$I_\pm = I_D(\Delta\varphi = \pm\eta_T/2). \tag{28}$$

If $a_1 L_F < 0$, to the δ determined from (27) should be added $-90°$. The details about adjusting the value of δ according to the experimental and geometrical parameters are given in §§ IV and V. For later discussion, the phase angle calculated from (27) is denoted as the nominal phase δ^*.

III. Experimental

An organic crystal of (2*R*, 3*R*)-3-acetoxy-5,7-dihydroxy-6-methylflavanone, $C_{18}H_{16}O_6$ (Fang, Chang & Cheng, 1987), was used for the experiments. The crystal is about 0·4 mm in diameter. The crystal belongs to the monoclinic system, space group $I121$, with four ($Z = 4$) molecules in the unit cell. The cell dimensions are $a = 14{\cdot}4881$, $b = 8{\cdot}0342$, $c = 14{\cdot}3406$ Å and $\beta = 110{\cdot}76°$ (Cheng, Cheng, Chang & Wang, 1989). The mosaic spread of the crystal measured from rocking curves is about 0·08°. The two-beam Bragg diffraction intensities were collected as usual by using an Enraf–Nonius CAD-4 diffractometer with Mo $K\alpha$ radiation. The moduli of the structure factors were deduced from the measured intensities. Those used for calculating $I_{K,T}$ are listed in Table 1. The crystal was then mounted on a Huber 400 semi-automatic goniometer to perform multiple diffraction experiments. An Elliott GX-21 rotating-anode X-ray generator was used. The details of the experimental set-up can be found in paper II. The beam divergence is about 0·03°. Fig. 1 shows the 101 multiple diffraction pattern obtained with Cu $K\alpha$ ($\lambda = 1{\cdot}541838$ Å) radiation. 101 is the primary *G* reflection. Multiple-diffraction *Umweg* peaks are indexed with the Miller indices of the secondary reflections *L*. Several indices sharing the same peak indicate the overlapping of several reflections including high-order *N*-beam ($N > 3$) diffractions. (Because of the relatively crowded peak distribution, not all of the peaks are labelled with their secondary reflections *L* in Fig. 1.) The origin, $\varphi = 0$, of the azimuthal rotation angle φ corresponds to the position at which the [010] direction coincides with the plane of incidence of the 101 reflection. The arrow shows the running direction of the paper chart. Fig. 2 shows part of the 303 multiple diffraction pattern for Cu $K\alpha$ radiation. All the multiple diffractions are of *Aufhellung* type. The uneven two-beam 303, as well as 101, reflection background is due to the boundary effect of the irregularly shaped crystal. The symmetry about $\varphi = 0$ of the two-beam intensity distribution visible in Figs. 1 and 2 indicates that the crystal shape is somewhat symmetric about the [010] direction.

Table 1. *Structure factors of* $C_{18}H_{16}O_6$ *for* Mo $K\alpha$ *radiation*

hkl	$\lvert F\rvert$	*hkl*	$\lvert F\rvert$
000	680	$20\bar{2}$	62
002	35	204	61
004	65	$\bar{2}04$	52
$0\bar{1}\bar{3}$	117	$2\bar{1}1$	35
015	30	$\bar{2}1\bar{1}$	35
$\bar{1}01$	96	$\bar{2}13$	53
$10\bar{1}$	96	$2\bar{2}\bar{2}$	80
101	4	$30\bar{3}$	49
$10\bar{3}$	27	303	103
103	265	$3\bar{1}\bar{2}$	102
105	5	$31\bar{2}$	102
112	138	$\bar{3}12$	102
114	88	402	18
$\bar{1}23$	47	$4\bar{1}\bar{1}$	29
200	14	$5\bar{1}4$	36

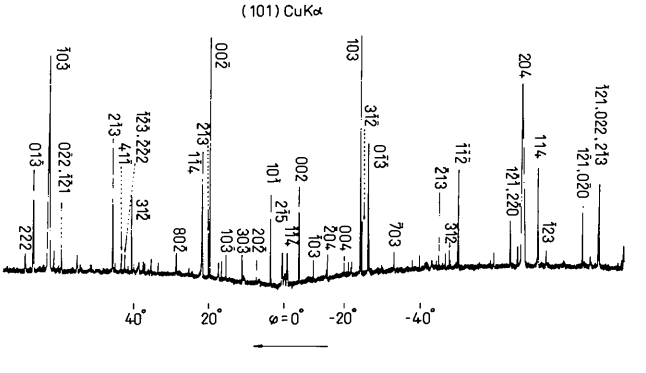

Fig. 1. Multiple diffraction (*Umweg*) pattern of 101 $C_{18}H_{16}O_6$ for Cu $K\alpha$ radiation ($\lambda = 1{\cdot}541838$ Å).

Step scan, I'_G *versus* $\Delta\varphi$, was carried out for each of the unoverlapped three-beam diffractions for 101 and 303 φ scans. The error in counting statistics for intensity measurements was kept less than 1%. Some of the step-scanned profiles $I'_G(\Delta\varphi)$ are shown, as examples, in Figs. 4 and 5 for *Umweg* and *Aufhellung*, respectively. The peak positions $\varphi_\pm$, defined as $\Delta\varphi = 0$, for each three-beam diffraction are determined according to equation (25) of paper I and the relation $\varphi_\pm = \varphi_0 \pm \beta_0$, where φ_0 is the initial azimuthal position of the reciprocal-lattice point L with respect to the plane of incidence of the primary G reflection. The peak intensities $I_P = I'_G(\Delta\varphi = 0)$ were recorded and the peak widths at half maxima were measured.

IV. Data analysis and phase determination

The scale factor C_0, as discussed in § II, can be determined from the $I_P/I_{K,T}(0)$ values of weak three-beam centrosymmetric diffractions *via* (22). For space group $I121$, hkl with $k = 0$ are centric reflections. The corresponding three-beam cases, $h0l/1-h,0,1-l$ and $h0l/3-h,0,3-l$) are also centric, where the indices before and after the slashes represent $L/G-L$. Table 2 lists the $I_{K,T}(0)$ and I_P values for the weakest reflections of the 101 and 303 scans. The two-beam intensities of 101 and 303 calculated according to (20) are also given. The $I_G^{(3)} - I_G^{(2)}$ values, which are proportional to $I_{K,T}(0)I_G^{(2)}$ are about 3×10^{-8} for the reflections of the 101 scan and 4×10^{-6} for the 303 scan. Since $I_G^{(3)} - I_G^{(2)}$ are very weak and $ql_0 < 1$ and $\mu l_0 \sim 10$ $(\text{cm}^{-1}) \times 0{\cdot}04\ (\text{cm}) = 0{\cdot}40$, it is justifiable to employ (18*a*) for the calculation of $I_{K,T}(0)$ for the reflections listed in Table 2. From Table 2 for the 101 scan, $30\bar{3}$, $\bar{2}04$, $\bar{3}12$ and $\bar{1}23$ reflections have $I_{K,T}(0)$ values ranging from 0·07 to 0·09. The centric three-beam reflections $30\bar{3}$ and $\bar{2}04$ were used to determine the scale factor C_0. As shown in Fig. (3*a*), the averaged C_0 is 6·87 with 8·28 and 5·60 as the upper and lower bounds, respectively. Since $30\bar{3}$ and $\bar{2}04$ are symmetry-related equivalent reflections, *i.e.* $30\bar{3}/\bar{2}04$ with respect to $\bar{2}04/30\bar{3}$, they are supposed to have the same $I_P/I_{K,T}(0)$ values. However, owing to the experimental errors, for example, the crystal boundary effects, the possible inhomogeneous intensity distribution of the incident beam and the crystal misalignment, $30\bar{3}$ and $\bar{2}04$ have slightly different values in $I_P/I_{K,T}(0)$. This difference is considered to be the principal error in C_0. The error in counting statistics is indicated as an error bar in Fig. 3. The

Table 2. *The* $I_{K,T}(0)$ *and* I_P *values for weak three-beam diffractions*

	L	$I_{K,T}(0)$	I_P
(*a*)	$G = 101\ [I_G^{(2)} \sim ql_0 \sim 4\times10^{-7}]$		
	$30\bar{3}$	0·070	0·553
	$\bar{2}04$	0·075	0·436
	$\bar{3}12$	0·072	0·480
	$\bar{1}23$	0·092	0·115
(*b*)	$G = 303\ [I_G^{(2)} \sim 8\times10^{-6}]$		
	$5\bar{1}4$	0·0022	0·021
	105	0·0033	0·019
	$20\bar{2}$	0·0052	0·024
	$3\bar{1}\bar{2}$	0·0061	0·005

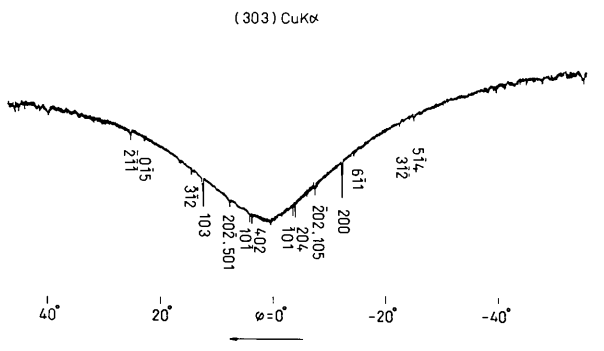

Fig. 2. Multiple diffraction (*Aufhellung*) pattern of 303 $C_{18}H_{16}O_6$ for Cu $K\alpha$ radiation.

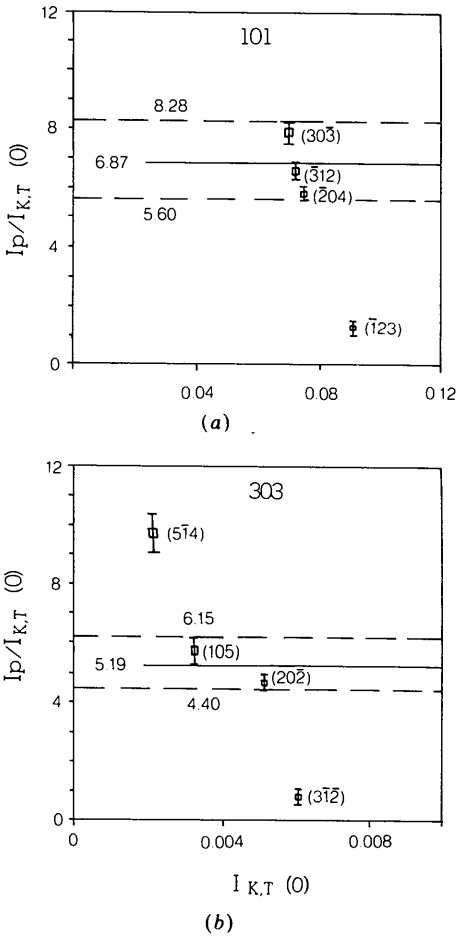

Fig. 3. Scaling for (*a*) 101 *Umweg* and (*b*) 303 *Aufhellung*.

mechanical backlash of the φ scan was checked to be very small. It has very little effect on the peak positions. The C_0 value obtained was then used to calculate the I_K for $\bar{3}12$ and $\bar{1}23$ reflections.

For the 303 scan, the centric three-beam reflections 105 and $20\bar{2}$ were used for the scaling (see Fig. 3*b*). The scale factor C_0 is equal to 5·19 with 6·15 and 4·40 as the upper and lower bounds. With this C_0 value, the I_K of $5\bar{1}4$ and $3\bar{1}\bar{2}$ reflections are calculated *via* (24).

The scaling shown in Figs. 3(*a*) and (*b*) also provides information about the enantiomorph (for example, see Ladd & Palmer, 1980) for acentric reflections. For *Umweg* (Fig. 3*a*), $\bar{1}23/2\bar{2}\bar{2}$ has $I_P/I_{K,T}(0)$ values less than the average C_0 value. This implies that the sign of sin δ^* is positive. For *Aufhellung* (Fig. 3*b*), the $I_P/I_{K,T}(0)$ of $5\bar{1}4/2\bar{1}\bar{1}$ is greater than while that of $3\bar{1}\bar{2}/015$ is less than C_0, *i.e.* the sign $S(\sin\delta^*)>0$ for $5\bar{1}4/2\bar{1}\bar{1}$ and $S(\sin\delta^*)<0$ for $3\bar{1}\bar{2}/015$.

The kinematical diffraction intensities $I_K(\Delta\varphi)$ are constructed according to (24) for acentric reflections. Figs. 4 and 5 show the constructed I_K, the experimental profiles I'_G and the dynamical profiles $I_D(=I'_G-I_K)$ for the 101 and 303 scans, respectively. The running direction of the paper chart is also indicated. The determined δ's from I_D *via* (27) are listed in Table 3 as δ^*'s, together with the signs, $S_\pm$, S_{GL}, $S_L(C)$, $S(\cos\delta)$, $S(\sin\delta)$ and $s(a_1)$, where

$$S(\cos\delta)=S(a_1)S(L_F)S_L(C)$$
$$=S(a_1)S_\pm S_{GL}S_L(C) \quad (29)$$
$$S(\sin\delta)=S(a_1)S(\sin\delta^*). \quad (30)$$

$S(a_1)$ is the sign of the polarization factor a_1. $S_L(C)$ is the sign defined from the asymmetry of the tails of the diffraction intensity profiles (Chang, 1982). The relation (30) is established based on (7) and (22). The δ^*'s are the nominal phases which need to be

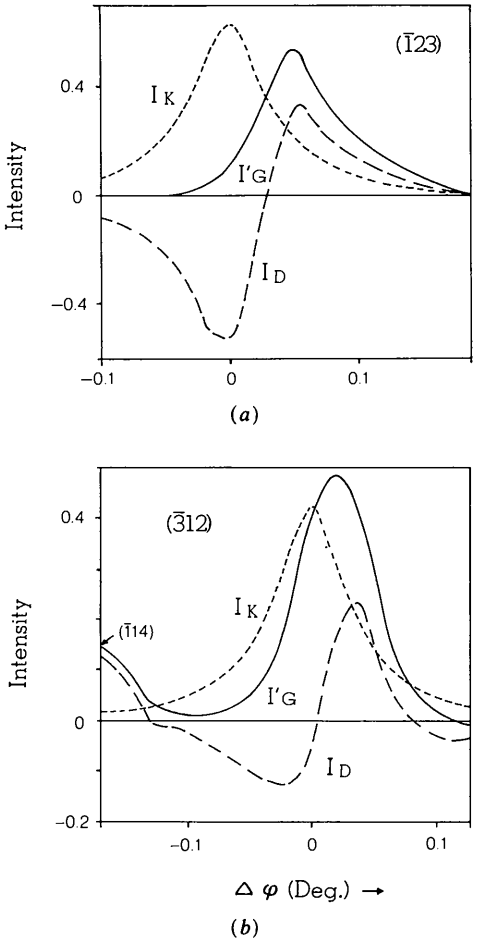

Fig. 4. Intensity profiles of I'_G, I_K and I_D for the 101 *Umweg*: (*a*) $\bar{1}23/2\bar{2}\bar{2}$ and (*b*) $\bar{3}12/4\bar{1}\bar{1}$ (the peak $\bar{1}14$ is nearby).

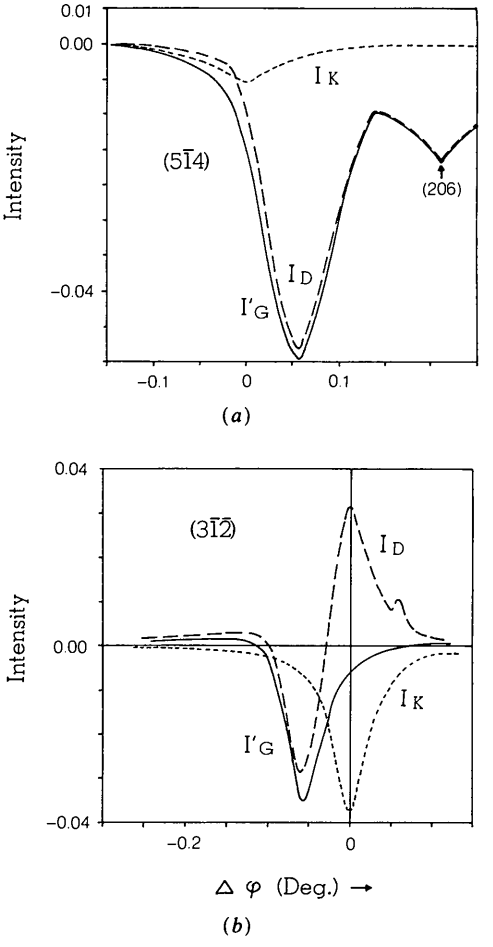

Fig. 5. Intensity profiles of I'_G, I_K and I_D for the 303 *Aufhellung*: (*a*) $5\bar{1}4/2\bar{1}\bar{1}$ (the peak 206 is nearby) and (*b*) $3\bar{1}\bar{2}/015$.

Table 3. *Experimentally determined phases for* $C_{18}H_{16}O_6$ ($\lambda = 1{\cdot}541838$ Å)

$L/G-L$	$S(a_1)$	$S_\pm$	S_{GL}	$S_L(C)$	$S(\cos\delta)$	$\delta^*(°)$	$S(\sin\delta)$	$\delta_E(°)$	$\delta_T(°)$
(*a*) 101 *Umweg* ($G=101$)									
$\bar{1}23/2\bar{2}\bar{2}$	+	+	+	+	+	26	+	26	23
$\bar{3}12/4\bar{1}\bar{1}$	+	+	+	−	−	181	−	181	171
$10\bar{1}/002$	+	+	+	+	+			0	0
$10\bar{3}/004$	+	+	+	+	+			0	0
$002/10\bar{1}$	+	+	+	+	+			0	0
$004/10\bar{3}$	+	+	+	+	+			0	0
$30\bar{3}/\bar{2}04$	+	−	+	−	−			180	180
$\bar{2}04/30\bar{3}$	+	−	+	−	−			180	180
(*b*) 303 *Aufhellung* ($G=303$)									
$5\bar{1}4/\bar{2}1\bar{1}$	+	+	+	−	−	136	+	136	132
$3\bar{1}\bar{2}/015$	+	+	+	−	−	−79	−	−169	−145
200/103	+	−	−	+	+				0
$105/20\bar{2}$	+	−	+	+	−				180
$\bar{1}01/402$	+	−	+	+	−				180
$204/10\bar{1}$	+	−	+	−	+				0
$402/\bar{1}01$	+	+	+	−	−				180
$10\bar{1}/204$	+	+	+	+	+				0
$20\bar{2}/105$	+	+	±	−	−				180
103/200	+	+	−	−	+				0

corrected according to the signs of $S(\cos\delta)$ and $S(\sin\delta)$. The corrected phases are listed as δ_E. The theoretical phases δ_T, calculated from the known atomic positions of the crystal, are also given.

The phases δ of those centric diffractions are also determined according to the signs of $\cos\delta$, $S(\cos\delta)$.

V. Discussion and concluding remarks

The main error in the determination of acentric phases comes from the errors in determining the C_0 value. From (21), the error $\Delta C_0/C_0$ is proportional to the sum of $\sum \Delta I_{K,T}/I_{K,T}$ and $\sum \Delta I_P/I_P$. The former is due mainly to the theoretical approximation and the extinctions and the latter results from the inaccuracy in the intensity measurements. Because of the crystal cell dimensions and the wavelength used, overlapping of multiple diffraction profiles is unavoidable. This overlapping certainly affects the intensity profiles and their positions. On the other hand, the irregular crystal boundaries cause complex dynamical excitation and the primary extinction which not only change the intensity distribution but also shift the peak position away from $\varphi_\pm$. Since the errors associated with $\Delta I_{K,T}$ and ΔI_P are not directly attainable, we can estimate the error $\Delta C_0/C_0$ only from the intensity variation of the two symmetry-related equivalent reflections and the counting statistics (see Fig. 3). The estimated $\Delta C_0/C_0$ is about ±20% for the *Umweg* and ±18% for the *Aufhellung*. The corresponding errors in the nominal phase δ^* determined *via* (27) are within ±5° for Lorentzian and Gaussian kinematical profiles for $\bar{1}23/2\bar{2}\bar{2}$, $5\bar{1}4/\bar{2}1\bar{1}$ and $3\bar{1}\bar{2}/015$ (Table 4). The errors in δ^* for $\bar{3}12/4\bar{1}\bar{1}$ are about ±25°. This is because the $I_P/I_{K,T}(0)$ value is so close to the C_0 value. Slight variation across C_0 may change the sign of δ^*, which will certainly cause a large error in δ^*. From Fig. 3(*a*), $\bar{3}12$ lies in between $30\bar{3}$ and $\bar{2}04$. This indicates that $\bar{3}12$ is practically a centric reflection.

Since we dealt with the weak diffractions from mosaic crystals, the effects of the phases on the intensity profiles are not obvious. To doubly check the determined phases, we use the asymmetry of the tails of the profile I'_G to determine the sign of $\cos\delta$ *via* (29) (Chang, 1982; Chang & Valladares, 1985). The experimental phase δ_E is then adjusted according to $S(\cos\delta)$ and $S(\sin\delta)$. For example, in Fig. 5(*b*), the nominal phase δ^* determined from the I_D curve is −79°. This contradicts the fact that $S(\cos\delta)<0$ and $S(\sin\delta)<0$, *i.e.* δ must be in the third quadrant. The experimental phase δ_E is therefore corrected to $-79-90°=-169°$. From Table 3, the maximum difference between δ_E and δ_T is about 25°.

It should be noted that the nominal phase δ^* is determined directly from the line profile I'_G obtained experimentally. The factors such as $S(a_1)$, $S_\pm$, S_{GL}, $S(\cos\delta)$ and $S(\sin\delta)$ have not been considered in calculating δ^*. The final experimental phase should therefore follow the relations given in (29) and (30) and should be adjusted to fit in the correct quadrant.

In deriving (18), we have adopted the expression for the diffracted intensity from the kinematical theory (Moon & Shull, 1964). Although the expression was originally derived for low extinction and weak reflections, its form, satisfying the theorem of reciprocity, seems to be quite general. A similar expression for the kinematical intensity has also been derived from the Takagi-Taupin equation for a parallelepiped crystal (Thorkildsen, 1987). The difference between the two is in the consideration of the crystal boundaries. In the present case, the extinc-

Table 4. *The determined nominal phases δ^* and the errors $\pm\Delta\delta^*$ corresponding to the lower and upper bounds of C_0*

L	$\delta^*(+\Delta\delta^*, -\Delta\delta^*)(^\circ)$ Lorentzian	Gaussian
(*a*) $G=101$		
$12\bar{3}$	26 (+3, −3)	40 (+3, −3)
$\bar{3}12$	181 (+22, −25)	159 (+26, −21)
(*b*) $G=303$		
$5\bar{1}4$	136 (+2, −1)	138 (+2, −2)
$3\bar{1}\bar{2}$	−79 (+5, −4)	−83 (+4, −3)

tion effects on the diffracted intensity are relatively small because the reflections involved are very weak. However, the crystal boundary seems to affect the intensity considerably. This can be seen directly from the comparison of the intensity backgrounds of the 101 and 303 φ scans.

The scaling factor C_0, defined in (21) to match the experimental and the theoretical kinematical intensities, has values greater than unity. The deviation of C_0 from unity is attributed to the theoretical approximation, extinctions and crystal boundary effects. Since extinction is small and (18) is valid for the present situation, the crystal boundary becomes the dominant effect. In paper II, plate-like crystals were used for the multiple-diffraction experiments. In that case, the crystal boundary is well defined. The corresponding peak intensity is proportional to the ratio of the direction cosines, γ_0/γ_L. C_0 is about 0·91 for Cu $K\alpha_1$ (see paper II). When γ_L approaches zero, the peak intensity I_P increases. It is therefore not surprising to have C_0 greater than unity when an irregularly shaped crystal is used.

The negative dynamical intensities I_D, shown in Figs. 4 and 5, represent the intensities which are taken away from the kinematical intensities I_K of the primary reflections and transferred to the secondary reflections *via* dynamical interaction. For $I_D>0$, the primary reflection gains intensity from the secondary reflection. This can be understood from the theoretical derivation and the calculated intensities given in paper I.

In paper I, we had adopted the term 'kinematical' for the intensity I_K which is independent of the reflection phases. This intensity is considered as the incoherent intensity. According to Kato (1980), by no means does the incoherent intensity result solely from the incoherent waves. Instead, coherent waves can also contribute to the incoherent intensity. Therefore, the 'kinematical' intensity I_K is attributed to both coherent and incoherent waves inside the crystal. Moreover, it is worth noting that, in the case of *Umweganregung*, the I_K derived from the fundamental equation of the wavefield, (2), has the same form as that from the kinematical theory.

The strength of the dynamical interaction which conveys the phase information in the multiply diffracted intensity distribution resulting from the coherent waves in the crystal depends, as stated in (1), on the parameter A. In order to increase the dynamical effect, strong reflections, long wavelengths and large crystals are ideal for the experiments. However, in practice, for irregularly shaped small crystals, compromised experimental conditions should be considered to reduce to minima the absorption, extinction and crystal boundary effects.

In conclusion, we have demonstrated that by modifying the expression for the kinematical intensity I_K with that derived from the kinematical theory and with the aid of crystal symmetry imposed by the space group, quantitative phase determination from weak three-beam diffraction can be achieved for mosaic crystals, with relatively large errors compared with that for perfect crystals. Further investigation is suggested to study the effects of crystal boundary on the intensity profiles of three-beam diffraction from noncentrosymmetric crystals so that improved precision in determining the phases is attainable.

The authors thank Y. Wang for providing the crystal sample and the two-beam diffraction data. The financial support from the National Science Council under contract No. NSC78-0208-M007-29 is also acknowledged.

References

CHANG, S.-L. (1982). *Phys. Rev. Lett.* **48**, 163-166.

CHANG, S.-L. (1984). *Multiple Diffraction of X-rays in Crystals*, p. 218. Berlin, Heidelberg, New York, Tokyo: Springer Verlag.

CHANG, S.-L. (1987). *Crystallogr. Rev.* **1**, 85-189.

CHANG, S.-L. & TANG, M.-T. (1988). *Acta Cryst.* A**44**, 1065-1072.

CHANG, S.-L. & VALLADARES, J. A. P. (1985). *Appl. Phys.* A**37**, 57-64.

CHENG, M.-C., CHENG, Y.-S., CHANG, C.-F. & WANG, Y. (1989). *Acta Cryst.* C**45**. In the press.

COLE, H., CHAMBERS, F. W. & DUNN, H. M. (1962). *Acta Cryst.* **15**, 138-144.

FANG, J. M., CHANG, C. F. & CHENG, Y. S. (1987). *Phytochemistry*, **26**, 2559-2561.

GONG, P. P. & POST, B. (1983). *Acta Cryst.* A**39**, 719-724.

HAN, F.-S. & CHANG, S.-L. (1983). *Acta Cryst.* A**39**, 98-101.

HØIER, R. & MARTHINSEN, K. (1983). *Acta Cryst.* A**39**, 854-860.

HÜMMER, K. & BILLY, H. W. (1986). *Acta Cryst.* A**42**, 127-133.

HÜMMER, K., WECKERT, E. & BONDZA, H. (1989). *Acta Cryst.* A**45**, 182-187.

JAGODZINSKI, H. (1980). *Acta Cryst.* A**36**, 104-116.

JURETSCHKE, H. J. (1982). *Phys. Rev. Lett.* **48**, 1487-1489.

KATO, N. (1980). *Acta Cryst.* A**36**, 770-778.

LADD, M. F. C. & PALMER, R. A. (1980). Editors. *Theory and Practice of Direct Methods in Crystallography*, p. 23. New York: Plenum Press.

MO, F., HAUBACK, B. C. & THORKILDSEN, G. (1988). *Acta Chem. Scand. Ser. A*, **42**, 130-138.

MOON, R. M. & SHULL, C. G. (1964). *Acta Cryst.* **17**, 805-812.

PINSKER, Z. G. (1977). *Dynamical Scattering of X-rays in Crystals*, Chap. 12. Berlin, Heidelberg, New York, Tokyo: Springer Verlag.
POST, B. (1977). *Phys. Rev. Lett.* **39**, 760-763.
SHEN, Q. (1986). *Acta Cryst.* A**42**, 525-533.
SHEN, Q. & COLELLA, R. (1988). *Acta Cryst.* A**44**, 17-21.
TANG, M.-T. & CHANG, S.-L. (1988). *Acta Cryst.* A**44**, 1073-1078.
THORKILDSEN, G. (1987). *Acta Cryst.* A**43**, 361-369.
ZACHARIASEN, W. H. (1945). *Theory of X-ray Diffraction in Crystals*. New York: John Wiley.